PHYSICAL REVIEW B VOLUME 50, NUMBER 12 15 SEPTEMBER 1994-II

Magnetic, transport, and structural properties of $Fe_{1-x}Ir_xSi$

B. C. Sales, E. C. Jones, B. C. Chakoumakos, J. A. Fernandez-Baca, H. E. Harmon, and J. W. Sharp
Oak Ridge National Laboratory, Oak Ridge, Tennessee 37831-6056

E. H. Volckmann
Marlow Industries, Dallas, Texas 75238

(Received 26 May 1994)

Magnetic susceptibility, resistivity, Seebeck, Hall, and powder x-ray and neutron-diffraction measurements were used to characterize single crystals of FeSi and polycrystalline samples of $Fe_{1-x}Ir_xSi$ for $x<0.2$. The Rietveld refinement of low-temperature powder neutron-diffraction data on FeSi showed no change in the space group and no structural anomalies from 4 to 300 K. Magnetic and transport data from 4 to 700 K are consistent with the characterization of FeSi as a narrow-gap semiconductor ($E_g=1200$ K) with strong intrasite correlations for the states just below and above the gap. Fits to the magnetic susceptibility and resistivity data suggest that the magnetic (or direct) gap may be larger than the transport (indirect) gap. Electron mobilities in FeSi are very low (3–5 $cm^2/V\,s$). The thermopower of FeSi has a large positive peak (500 $\mu V/K$) at 50 K that is attributed to an unusually strong phonon-drag mechanism. Iridium acts as an electron donor in the $Fe_{1-x}Ir_xSi$ alloys. As the iridium doping level is increased, there is a rapid decrease in the low-temperature resistivity and a large negative (-140 $\mu V/K$) phonon-drag contribution to the thermopower. For Peltier cooling applications, a maximum value for ZT of 0.07 was found for a $Fe_{0.95}Ir_{0.05}Si$ alloy at 100 K.

I. INTRODUCTION

The compound FeSi crystallizes in the cubic B20 structure (space group P213), which has eight atoms per unit cell. In spite of this relatively simple crystal structure, a complete understanding of the magnetic and transport properties of FeSi has remained elusive for over 30 years.[1-7] Recently, it has been noted that some of the magnetic and transport properties of FeSi are similar to those exhibited by an unusual class of rare-earth compounds such as SmB_6 $CeFe_4P_{12}$, $Ce_3Bi_4Pt_3$, and YbB_{12}.[8,9] For these rare-earth compounds, it is thought that the hybridization between the localized $4f$ electrons and an itinerant band results in the formation of a narrow-gap semiconductor. The ability of the $4f$ electrons to hybridize with the conduction band in this manner depends on the proximity of the $4f$ level to the Fermi energy, which in turn is related to the ability of the rare-earth ion to exist in two different valence states. A narrow-gap semiconductor is formed only if the hybridized band has an even number of electrons and if no other bands cross the Fermi level; otherwise a mixed-valence metal results. However, if a gap is formed by this type of hybridization, the electronic states near the bottom (top) of the conduction (valence) band are an unusual superposition of extended band states and highly correlated ioniclike states.

Figure 1 shows schematically how a gap might be formed in FeSi as a result of hybridization between a localized $3d$ level and an extended conduction band. It is surprising, however, that such a picture is valid for a concentrated $3d$ compound such as FeSi since the spatial extent of the $3d$ wave functions normally results in a rather broad $3d$ band. The concept of assigning a formal valence to Fe in FeSi is also unexpected since the small electronegativity difference between iron and silicon would suggest a highly covalently bonded material. In spite of these objections, the experimental data on FeSi are described, at least qualitatively, by the physics depicted in Fig. 1.

The present investigation of undoped and doped FeSi materials was motivated by a desire to understand the physics of these materials and to determine whether this unusual narrow-gap semiconductor could be used in thermoelectric refrigeration applications. The efficiency of a thermoelectric refrigerator is determined by the dimensionless parameter ZT, where T is the temperature and Z the coefficient of merit is given by

$$Z=S^2/\rho\kappa\ , \tag{1}$$

where S is the thermopower or Seebeck coefficient, ρ is the electrical resistivity, and κ is the thermal conductivity. For a practical Peltier refrigerator, a good value for ZT at $T=100$ K would be 1. Traditionally, a good candidate material for Peltier cooling is a semiconductor with an energy gap that is at least 10 times larger than the desired maximum operating temperature (i.e., $E_g>10k_BT$),[10,11] is composed of heavy elements with small differences in electronegativity, and has a crystal structure containing a large number of atoms per unit cell. If the gap is too small, then at the higher operating temperatures intrinsic electron and hole currents are created drastically decreasing the thermopower. Small differences in electronegativity *usually* result in high electron or hole mobilities, and a complicated crystal structure composed of heavy elements often results in a low thermal conductivity.[12] In addition, it has been shown[13,14] that for normal semiconductors maximizing Z

0163-1829/94/50(12)/8207(7)/$06.00 ©1994 The American Physical Society

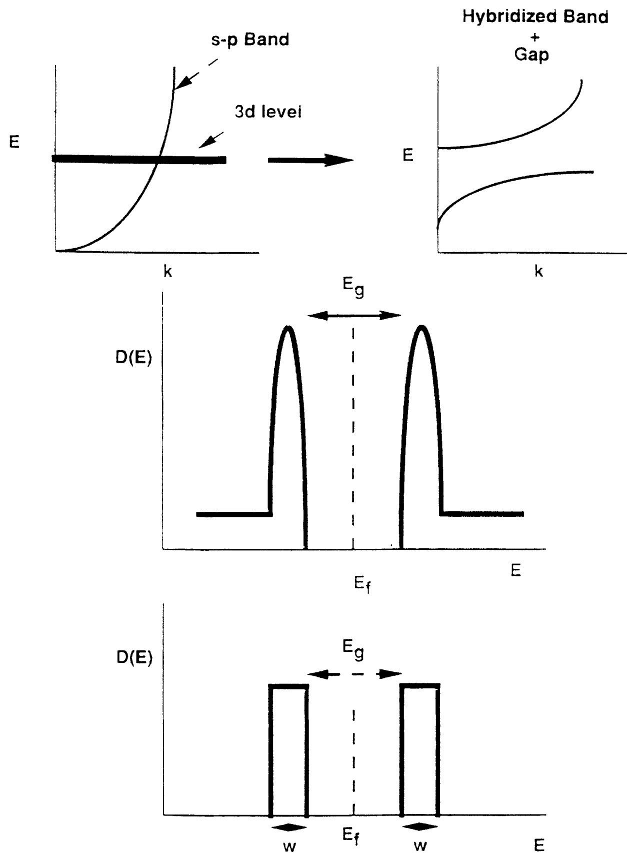

FIG. 1. Schematic of the formation of a hybridization gap in FeSi. At the bottom of the figure is the simplified band structure used to calculate the magnetic susceptibility and resistivity.

is equivalent to maximizing a parameter B given by

$$B=\mu(m^*/m_0)^{3/2}/\kappa_L \ , \tag{2}$$

where μ is the carrier mobility, m^* is the effective band mass, m_0 is the free-electron mass, and κ_L is the lattice contribution to the thermal conductivity. Peltier materials currently in use have large mobilities (>1000 $cm^2/V\,s$), but relatively small band masses ($m^*/m_0<1$).

II. EXPERIMENT

A large single crystal (3.5 cm in diameter by 7 cm long) of FeSi was grown using the Czochralski method. Stoichiometric quantities of 99.99% vacuum remelted iron (Johnson-Matthey) and semiconductor grade Si (99.999%) were rf melted in a high-purity (99.9%) alumina crucible that snugly fit into a graphite crucible. A small bar of high-purity iron was used as a seed for the initial nucleation of the FeSi crystal. The pulling head with the iron seed and the alumina crucible containing the molten FeSi were rotated in opposite directions at approximately 20 rpm. The crystal was pulled at approximately 1 cm/h in an argon atmosphere. The crystal was sliced using an electric spark saw along desired crystallographic directions for the various transport measurements. Approximately 2 cm^3 of the crystal was ground into a powder for powder-neutron diffraction experiments. Polycrystalline samples of undoped and doped FeSi were prepared by rf melting stoichiometric quantities of the starting elements in an alumina crucible in an argon atmosphere. All samples were rf melted at least twice. This preparation procedure was chosen over simply arc melting the elements on a water-cooled copper hearth because of the ability to cool the rf-heated samples more slowly which reduced the cracking of the polycrystalline buttons. The lattice constant and phase purity of all samples were checked using a SCINTAG automated diffractometer with an intrinsic Ge detector using Cu K_α radiation. Low-temperature powder neutron-diffraction data from FeSi were collected using the diffractometer at the High Flux Isotope Reactor at the Oak Ridge National Laboratory. For some samples, polished cross sections were examined with an optical microscope using polarized light.

Electrical resistivity and thermopower measurements were made from 6 to 700 K using an automated closed-cycle refrigerator system (6–300 K) and an automated high-temperature furnace system (300–1000 K). Both systems were operated in vacuum and were interfaced to a Macintosh computer using Labview hardware and software. Typical sample dimensions were $0.15\times0.15\times1.3$ cm^3. Resistivity measurements were made using a standard four-probe dc measurement configuration with typical currents of 10 mA, the polarity of which was reversed for each datum point. A small heater near one end of the sample provided a thermal gradient (typically 4–6 K) for the Seebeck measurements. The Seebeck voltage and temperature difference were measured with 0.0076-cm Cu wires and 0.0127-cm type-E thermocouples, respectively, that were attached to the sample with conducting silver paint. The reported Seebeck coefficients are with respect to copper metal. Both the high-temperature and low-temperature measurement systems were calibrated using high-purity Pt and Pd standards. Hall measurements from 4 to 300 K were made in a separate cryostat in fields as high as 8 T. Magnetic susceptibility and magnetization curves were made from 4 to 1000 K with a Faraday system using Lewis coils and a cryostat/furnace obtained from George Associates. The Faraday system was calibrated using a National Institute of Standards and Technology MnF_2 standard. On selected samples, thermal conductivity values were estimated using a modification of the Harman method.[15]

III. RESULTS AND DISCUSSION

A. Cell parameters and phase purity

The lattice constant versus temperature for FeSi is shown in Fig. 2(a) as determined from powder neutron-diffraction data. There is a smooth variation of the lattice constant with temperatures from 20 to 300 K, indicating that FeSi does not undergo any structural transformation in this temperature regime. This finding is in agreement with previous reports in the literature.[1] In a preliminary report, we observed a small discontinuity in

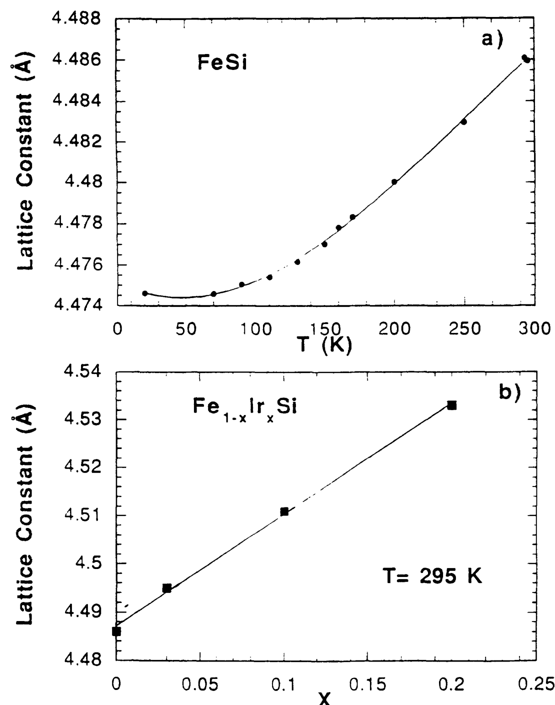

FIG. 2. Lattice constant versus temperature for FeSi (top) and lattice constant versus composition (bottom) for iridium-doped FeSi. The error bars are about the size of the datum points.

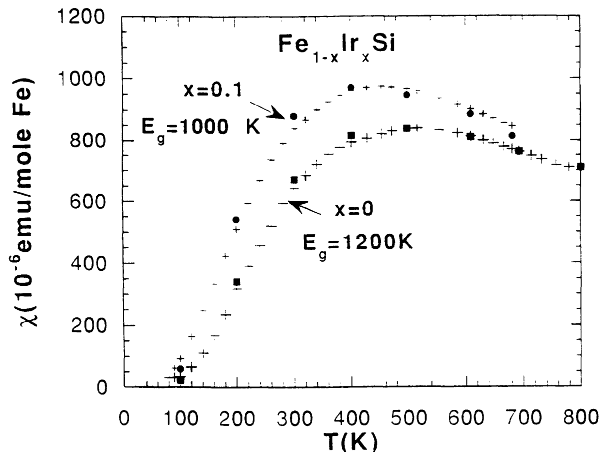

FIG. 3. Magnetic susceptibility versus temperature for FeSi and $Fe_{0.9}Ir_{0.1}Si$. The crosses are the experimental data points and the solid circles and squares are the values calculated using the simple two-band model described in the text with a width for each band of $W=300$ K and the values for E_g, as shown in the figure.

the lattice constant at 115 K,[16] but more careful measurements indicated that this anomaly was an experimental artifact. Rietveld refinements of the diffraction data failed to show any evidence of a second phase. Optical study of polished sections of the FeSi single crystal also failed to show any definitive evidence of impurity phases. The effects of Ir doping on the lattice constant are shown in Fig. 2(b) and are much larger than the variation of the cell constant with temperature. The linear dependence of the cell constant on concentration is an indication that the iridium successfully replaces the iron in the FeSi structure, at least up to $x=0.2$. The compound IrSi crystallizes in a hexagonal structure.

B. Magnetic properties

The magnetic susceptibility versus temperature is shown in Fig. 3 for the FeSi single crystal and a polycrystalline sample of $Fe_{0.9}Ir_{0.1}Si$. The single-crystal susceptibility data have been corrected for a small quantity of ferromagnetic iron (0.04%) and paramagnetic iron (0.1%). The paramagnetic correction only affected data below 100 K, and the ferromagnetic contribution to the high field susceptibility was only about 5% at room temperature. A small quantity of either antisite or interstitial iron defects in the crystal could account for the small additional contributions to the susceptibility. For the Ir-doped sample, the susceptibility was corrected for a paramagnetic iron component that corresponded to about 1.5% Fe. This was a significant correction which amounted to about 20% of the susceptibility at room temperature. Without this correction, the raw susceptibility data for the $Fe_{0.9}Ir_{0.1}Si$ sample passes through a minimum of 7×10^{-4} emu/mole Fe at 120 K. The substitution of Ir for Fe clearly changes the local environment of some of the iron atoms in the material to produce a paramagnetic ground state for these iron atoms. If enough of these magnetic atoms are produced with higher Ir doping, some type of magnetic order could result, such as the helimagnetic state found in $Fe_{1-x}Co_xSi$ alloys[17] or perhaps a spin glass. The magnetic behavior of FeSi doped with higher concentrations of Ir was not investigated in the present work, but might prove interesting since Ir, unlike Co, is not expected to form a local magnetic moment, which might make the results simpler to interpret. Any ordered magnetic state would then have to be associated with the iron moments or bands.

As pointed out by Jaccarino *et al.*[3] the magnetic properties of FeSi can be understood either by involving extremely narrow "*d*-like" bands such as depicted in Fig. 1, or using a simple "free-ion-like" model with a nonmagnetic ground state ($S=0$) and a magnetic excited state. The band model is somewhat more flexible, however, since the same model can be used to examine both the magnetic and transport data. If the two peaks in the density of states near the gap (Fig. 1) are modeled using two rectangular bands of width W separated by a gap E_g, the correct temperature dependence of the FeSi susceptibility (Fig 3) is obtained with $W=300$ K for each band and $E_g=1200$ K. To quantitatively fit the susceptibility data, however, each band must be normalized to contain about four (3.75) electrons (two spin-up and two spin-down electrons per band). On the other hand, if each band is restricted to a normalization of one electron per band, the susceptibility data can also be fit by assigning each

fermion in the band a magnetic moment of $1.93\mu_B$. These results simply reflect the importance of intrasite Coulomb interactions in the formation of the hybridized band. The corrected susceptibility for the $Fe_{0.9}Ir_{0.1}Si$ alloy (Fig. 3) can be fit using the same bandwidth (300 K) and normalization (3.75 electrons per band) but with E_g lowered to 1000 K.

The value of the gap obtained from fitting the susceptibility data of pure FeSi (1200 K or 834 cm^{-1}) is very close to the energy (about 800 cm^{-1}) at which a rapid decrease in the electrical conductivity $\sigma_1(\omega)$ begins in infrared reflection data.[7] This onset may reflect the value for the direct gap in FeSi, which theory suggests[18] should be somewhat larger than the indirect gap measured in transport experiments.

C. Transport properties of FeSi

The resistivity data for the FeSi single crystal from 4 to 700 K are shown in Fig. 4 and are in good agreement with all previous measurements on FeSi single crystals. "Semiconducting behavior" ($d\rho/dT<0$) is found from 4.2 up to 340 K, while above 340 K a "metallic" resistivity ($d\rho/dT>0$) is observed. The resistivity shown in Fig. 4, however, is exactly what would be expected for a narrow-gap semiconductor. At low temperatures the decreasing carrier concentration dominates and $d\rho/dT<0$, while at temperatures where $k_BT\cong E_g/3$, the temperature dependence of the scattering dominates and $d\rho/dT>0$. Above about 50 K the temperature dependence of the scattering can be often approximated as a power law of the form T^b.[19] The electrical conductivity then is given by

$$\sigma=1/\rho=AT^{-b}n(T)\ , \tag{3}$$

where n is the concentration of electrons or holes, and A is a constant.

To obtain the simplest possible model for the electrical conductivity of FeSi, the band structure shown in Fig. 1 is used, the same carrier mobility is assumed for both electrons and holes, and the classical temperature dependence of the mobility due to phonon scattering is adopted ($b=1.5$).[19] Using the same parameters for the bandwidths (300 K) and band gap (1200 K) that were used to fit the susceptibility data, the resistivity was calculated with the constant A adjusted to give the correct value for the resistivity at 300 K. A comparison between this simple model (filled circles) and the FeSi data is shown in the lower panel of Fig. 4. Qualitatively, the agreement is surprisingly good considering the crude approximations. On the basis of a theoretical model[18] which describes the formation of the hybridization gap, the indirect gap appropriate for the transport measurements may be smaller than the direct gap measured in an optical or magnetic measurement. To test this hypothesis, the resistivity data for FeSi above 50 K were fit to Eq. (3), but both E_g and b were allowed to vary. Almost a quantitative fit to the data is obtained when $E_g=600$ K and $b=0.85$, which suggests that the transport gap is about half of the magnetic gap.

The Hall data for the FeSi single crystal are shown in Fig. 5 as the "apparent" carrier concentration versus temperature. At room temperature, the apparent carrier concentration is found to be 2×10^{22} electrons/cm^3, a value characteristic of a compensated semiconductor. The presence of substantial quantities of both electron and holes at room temperature is expected in FeSi because of the small energy gap. At 20 K, the apparent carrier concentration of 3×10^{19} electron/cm^3 is attribut-

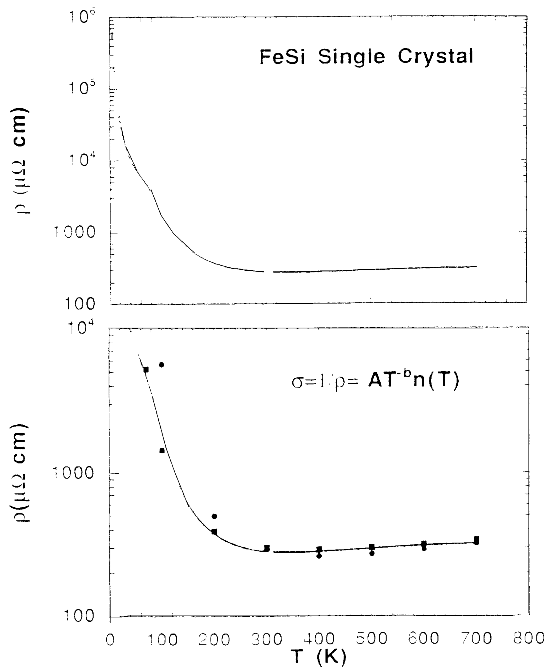

FIG. 4. Electrical resistivity versus temperature for an FeSi single crystal from 4 to 700 K (top) and the same resistivity data fit from 50 to 700 K using the simple two-band model described in the text (bottom) with a width for each band of $W=300$ K. The solid circles correspond to $E_g=1200$ K and $b=1.5$, while the solid squares correspond to $E_g=600$ K and $b=0.85$. The better fit to the resistivity data with a value for E_g of 600 K (about half the optimum value found from fitting the susceptibility data) suggests that the transport gap is less than the direct gap measured in a magnetic or optical experiment.

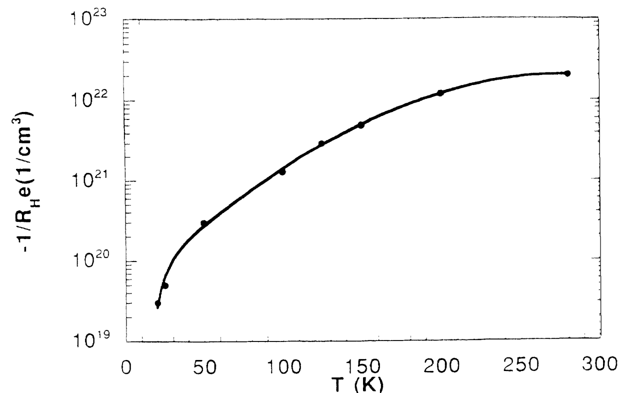

FIG. 5. "Apparent" carrier concentration, as determined from Hall data, versus temperature.

ed to extrinsic doping of this amount. Combining the low-temperature Hall data with the resistivity data shown in Fig. 4 gives values for the electron mobility of 3–5 cm^2/V s. These values are extremely low in comparison with "normal" narrow-gap semiconductor carrier mobilities of 100–10 000 cm^2/V s, but are comparable to values found for rare-earth hybridization compounds.[8] Low values of the mobility for carriers in FeSi also are not expected because of the small difference in electronegativity between Fe and Si. However, low mobility and high effective mass are expected for carriers that reside in the type of band structure depicted in Fig. 1. Referring to Eq. (2), for FeSi to be a viable material for thermoelectric refrigeration, the low mobility of the carriers would have to be compensated by an unusually high effective band mass.

The Seebeck coefficient from 6 to 700 K for the FeSi crystal is shown in Fig. 6. These data are in good agreement with previous thermopower data reported by Wolfe, Wernick, and Hazko.[2] The large positive peak in the thermopower at 50 K is probably due to a phonon-drag mechanism. When the electron-phonon scattering rate becomes comparable to or larger than the phonon-phonon scattering rate, thermal equilibrium among the phonons becomes tied to equilibrium among the electrons. If the electrons (or holes) are drifting due either to a temperature gradient or an electrical current, the phonons are "dragged" along.[20] The phonon-drag peak normally occurs in the 50–80 K temperature range. Above this temperature, the phonons increasingly relax via umklapp scattering and hence S should decrease as T^{-1} for $T > T_{peak}$. At low temperatures the heat capacity of the phonons decreases as T^3 (Debye model), which implies that for $T < T_{peak}$, S should decrease as T^3. For many materials, including some of the doped FeSi alloys discussed in Sec. III D, the peak in S approximately follows this classic behavior.

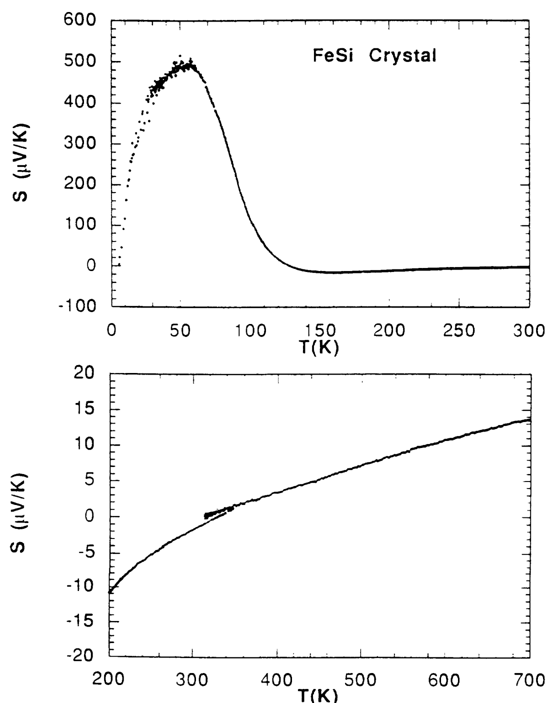

FIG. 6. Seebeck coefficient versus temperature for the FeSi single crystal.

Low-temperature infrared reflection measurements on an FeSi single crystal by Schlesinger *et al.*[7] showed the presence of several extremely strong and well-defined optical phonons. For example, the phonon at 332 cm^{-1} had a strength of 1300 cm^{-1}, which is larger than that of the strongest infrared-active phonon in MgO. Such strong phonon modes are clearly related to the large magnitude ($S = 500$ μV/K) of the phonon-drag peak in FeSi. The shape of the peak, however, does not follow the expected phonon-drag temperature dependence either above or below the maximum in S. This may be because of the discrete nature of the strong phonon modes (non-Debye-like spectrum) in pure FeSi.

Although at low temperatures most of the carriers are electrons, the positive sign of the phonon-drag peak suggests that the remaining holes interact more strongly with the phonons. At temperatures just above the "phonon-drag" peak, the carriers are still predominantly electrons (from Hall data) and hence S becomes negative. As the temperature is increased further, intrinsic electrons and holes are excited. If the holes have a slightly higher mobility than the electrons in FeSi, eventually the holes will dominate the thermopower and S will once again become positive. This appears to occur near room temperature. The roughly linear increase in S for $T > 300$ K is characteristic of a heavily doped semiconductor or a metal.

Thermal conductivity measurements on a single crystal of FeSi were reported by Krentsis, Ostrovskii, and Gel'd.[6] They found that the thermal conductivity of FeSi increased from 10 W/m K at room temperature to a value of 25 W/m K at 60 K. These values are about 10 times larger than typical "good" values for Peltier refrigeration materials. Combining these data for the thermal conductivity with the present data for FeSi (Figs. 4 and 6) yields a maximum value for ZT at 70 K of 0.015, considerably less than the desired value of 1. It is well known, however, that alloying can substantially decrease the lattice contribution to the thermal conductivity, and these effects are investigated in the next subsection.

D. Properties of doped FeSi

A variety of elements were substituted for either Fe or Si in FeSi in order to increase the extrinsic carrier concentration at low temperatures, increase the electrical conductivity, and decrease the lattice contribution to the thermal conductivity. Whether a particular dopant element resulted in either electron or hole doping depended primarily on the number of electrons outside the noble-gas core rather than on the formal valence of the element. For example, elements in the same column of the Periodic Table as Fe (Os and Ru) had the least effect on the transport properties, elements in the column to the right of Fe(Co, Rh, and Ir) acted as electron donors, while elements to the left of Fe tended to act as hole donors, al-

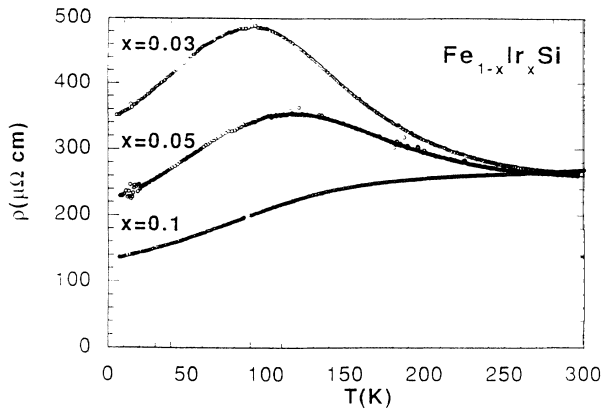

FIG. 7. Resistivity versus temperature for three of the $Fe_{1-x}Ir_xSi$ alloys.

though Re may be an exception. Similar results were found with substitutions for Si.

Of the various elements substituted for iron, iridium produced the most rapid decrease in electrical conductivity for a given doping level. As shown in Fig. 7, an Ir concentration of 3% ($Fe_{0.97}Ir_{0.03}Si$) dramatically decreased the maximum resistivity to a value of about 500 $\mu\Omega$ cm at 90 K. To get a similar decrease in the resistivity with Rh or Co doping required about twice the doping concentration. For the three Ir concentrations shown in Fig. 7 (0.03, 0.05, and 0.10), only the low-temperature values of the resistivity are affected by the doping. At room temperature, all three polycrystalline samples have the same value for the resistivity of 260±20 $\mu\Omega$ cm, indicating the dominance of thermally excited intrinsic carriers and no mobility loss due to the dopant.

The temperature dependence of the Seebeck coefficients for the iridium-doped samples are shown in Fig. 8. Note that the Seebeck coefficient is negative, consistent with extrinsic electron doping by iridium substitution for iron. In addition to the negative sign, the position of the peak is 20–30 K higher than found for pure FeSi and the peak shape is somewhat broader. The Seebeck data from 100–300 K for the $Fe_{0.97}Ir_{0.03}Si$ and $Fe_{0.95}Ir_{0.05}Si$ samples are linear in T^{-1}, which suggests that the negative peak in S for these alloys is due to a phonon-drag mechanism caused by the interaction of the extrinsic electron carriers and the phonons. None of the data below 50 K follow a T^3 law, although with the present experimental equipment accurate Seebeck measurements are only obtained at temperatures above 20 K because of the limited sensitivity of type-E thermocouples.

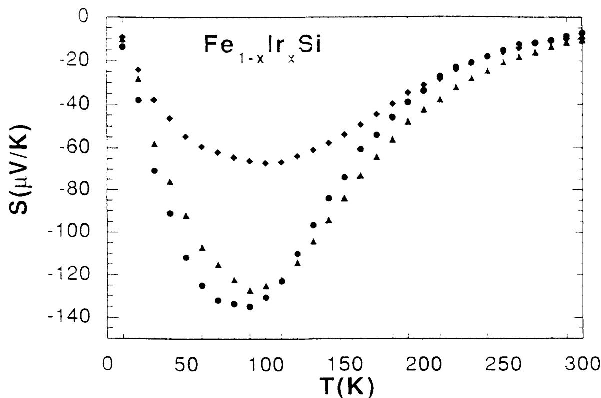

FIG. 8. Seebeck coefficient versus temperature for three $Fe_{1-x}Ir_xSi$ alloys: diamond, $x=0.10$; triangle, $x=0.05$; and circle, $x=0.03$.

Figure 9 shows an example of extrinsic hole doping in an $FeSi_{0.9}Al_{0.1}$ alloy. The resistivity of $FeSi_{0.9}Al_{0.1}$ is similar to the resistivity of the $Fe_{0.95}Ir_{0.05}Si$ alloy shown in Fig. 8. The Seebeck coefficient, however, is positive over the entire temperature range, indicating that replacing Si with Al has added extrinsic holes.

Of the various dopants introduced into FeSi, Ir appeared to be the most promising with respect to thermoelectric refrigeration. The low-temperature thermal conductivity of the $Fe_{0.95}Ir_{0.05}Si$ alloy (which had the largest value of S^2/ρ) was measured using a modification of the Harman method.[15] This method relies on the Peltier effect to produce a temperature gradient across an appropriately mounted sample. Although microcracking of the brittle $Fe_{0.95}Ir_{0.05}Si$ alloy presented some problems during these measurements, it was estimated that the maximum value of ZT at 100 K was about 0.07, which implies a thermal conductivity of about 7.5 W/m K at 100 K (3 times smaller than the thermal conductivity of pure FeSi at the same temperature). The maximum ZT of the Ir-doped FeSi alloy is about 5 times larger than the maximum ZT for undoped FeSi, but another factor of 10

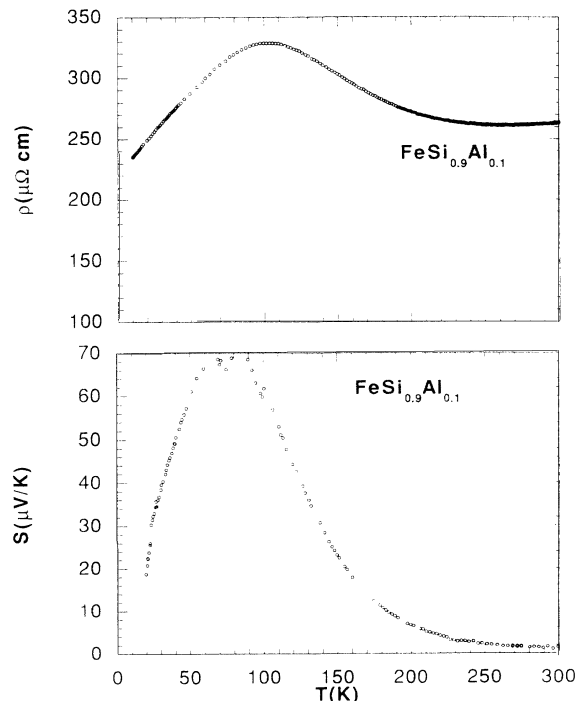

FIG. 9. Resistivity (top) and Seebeck coefficient (bottom) versus temperature for the hole-doped $FeSi_{0.9}Al_{0.1}$ alloy.

improvement in ZT is required before these materials would be of use for Peltier refrigeration applications in the liquid-nitrogen temperature range.

IV. CONCLUSIONS

The magnetic and transport data from FeSi and $Fe_{1-x}Ir_xSi$ alloys are consistent with the description of FeSi as a narrow-gap semiconductor with formation of the gap caused by hybridization between localized $3d$ levels and an itinerant conduction band. The magnetic susceptibility and the resistivity data of FeSi can be fit using the simplified band model shown at the bottom of Fig. 1 with $W=300$ K and $E_g=1200$ K. The value of the gap obtained from fitting the susceptibility data of pure FeSi (1200 K or 834 cm^{-1}) is close to the onset energy (about 800 cm^{-1}) where infrared reflection data begin to exhibit a rapid decrease in the electric conductivity $\sigma_1(\omega)$.[7] A somewhat better fit to the resistivity measurements was obtained, however, if $E_g=600$ K. This may be an indication, as suggested by theory,[18] that the direct gap in FeSi measured in a magnetic susceptibility experiment is larger than the indirect gap measured in transport experiments. Neither FeSi nor $Fe_{1-x}Ir_xSi$ alloys exhibited much promise as materials for low-temperature Peltier refrigeration. The largest value of ZT was obtained for an $Fe_{0.95}Ir_{0.05}Si$ alloy and was 0.07 at 100 K, which is about an order of magnitude too low.

ACKNOWLEDGMENTS

This research was sponsored in part by a Cooperative Research and Development Agreement, Contract No. ORNL92-0116, in part by the Oak Ridge Institute for Science Education, and in part by the Division of Materials Sciences, U.S. Department of Energy under Contract No. DE-AC05-84OR21400 with Martin Marietta Energy Systems, Inc.

[1]G. K. Wertheim, V. Jaccarino, J. H. Wernick, J. A. Seitchik, H. J. Williams, and R. C. Sherwood, Phys. Lett. **18**, 89 (1965).

[2]R. Wolfe, J. H. Wernick, and S. E. Hazko, Phys. Lett. **19**, 449 (1965).

[3]V. Jaccarino, G. K. Wertheim, J. H. Wernick, L. R. Walker, and S. Arajis, Phys. Rev. **160**, 476 (1967).

[4]S. Takagi, H. Hiroshi, S. Ogawa, and J. H. Wernick, J. Phys. Soc. Jpn. **50**, 2539 (1981).

[5]G. Shirane, J. E. Fischer, Y. Endoh, and K. Tajima, Phys. Rev. Lett. **59**, 351 (1987).

[6]R. P. Krentsis, F. I. Ostrovskii, and P. V. Gel'd, Fiz. Tekh. Poluprovodn. **4**, 403 (1970) [Sov. Phys. Semicond. **4**, 339 (1970)].

[7]Z. Schlesinger, Z. Fisk, H.-T. Zhang, M. B. Maple, J. F. DiTusa, and G. Aeppli, Phys. Rev. Lett. **71**, 1748 (1993).

[8]Z. Fisk, P. C. Canfield, J. D. Thompson, and M. F. Hundley, J. Alloys Compounds **181**, 369 (1992).

[9]G. Aeppli and Z. Fisk, Comments Condens. Matter Phys. **16**, 155 (1992).

[10]G. D. Mahan, J. Appl. Phys. **65**, 1578 (1989).

[11]J. O. Sofo and G. D. Mahan, Phys. Rev. B **49**, 4565 (1994).

[12]G. A. Slack, Solid State Phys. **34**, 1 (1979).

[13]R. P. Chasmar and R. Stratton, J. Electron. Control **7**, 52 (1959).

[14]A. F. Ioffe, *Semiconductor Thermoelements and Thermoelectric Cooling* (Infosearch Limited, London, 1957).

[15]T. C. Harman, J. H. Cahn, and M. J. Logan, J. Appl. Phys. **30**, 1351 (1959).

[16]B. C. Sales, E. C. Jones, B. C. Chakoumakos, J. A. Fernandez-Baca, and H. E. Harmon, Bull. Am. Phys. Soc. **39**, 732 (1994).

[17]J. Beille, J. Voiron, and M. Roth, Solid State Commun. **47**, 399 (1983).

[18]P. Riseborough, Bull. Am. Phys. Soc. **39**, 56 (1994).

[19]J. M. Ziman, *Principles of the Theory of Solids* (Cambridge University Press, Cambridge, England, 1964), p. 194.

[20]P. M. Chaikin, in *Organic Superconductivity,* edited by V. Z. Kresin and W. A. Little (Plenum, New York, 1990), p. 101.